

---

# PHASE-MODULATED PARAMETRIC ANTI-STOKES STIMULATED RAMAN SCATTERING OF CHERENKOV-TYPE IN SELF-FOCUSING AREAS OF EXCITING RADIATION

A.I. IVANISIK,<sup>1</sup> O.IU. ISAIENKO,<sup>1</sup> P.A. KOROTKOV,<sup>1</sup> G.V. PONEZHA<sup>2</sup>

<sup>1</sup>Taras Shevchenko National University of Kyiv, Radiophysics Faculty  
(4g Bldn., 2, Academician Glushkov Ave., Kyiv 03127, Ukraine; e-mail: aivan@univ.kiev.ua)

<sup>2</sup>National Academy of Statistics, Accounting and Auditing  
(1, Pidhirna Str., Kyiv 04107, Ukraine)

PACS 42.65.Dr  
©2012

---

The influence of the speed of the focal point under self-modulation of the phase and self-focusing on the frequency-angular radiation spectra of a parametric stimulated Raman scattering (SRS) anti-Stokes component is considered. The phase self-modulation of both exciting and scattered anti-Stokes radiation is taken into consideration. The creation of broadened anti-Stokes frequency-angular bands is explained. The most intense frequency-angular bands, which are described by relations typical of the Cherenkov radiation, are generated when the speed of the self-focused focal point coincides with the phase velocity of a nonlinear polarization at the anti-Stokes Raman frequency and the phase velocity of a scattered axial radiation. In particular, under the excitation by nanosecond laser pulses, such bands in toluene reach shifts of  $\approx -200 \text{ cm}^{-1}$  relatively to the anti-Stokes Raman frequency.

This creates a situation similar to the one, in which the Vavilov–Cherenkov radiation is observed.

In practical and theoretical aspects, SF creates a new situation that is impossible or difficult to achieve under other conditions and by other technical methods.

Thus, unlike the usage of conventional lenses, the focal area length  $b$  varies from  $\sim 0.1$  to 10 mm at the radius of  $\sim 5 \mu\text{m}$ . The duration of the self-focused laser radiation action on the medium at a fixed point is  $\sim b/v_{\text{fp}}$ . When the speed of a focal point becomes superluminal, the duration of the action  $b/v_{\text{fp}}$  at the minimum length  $b$  decreases to the femtosecond interval even for nanosecond exciting laser pulses.

When there is no SF, the group velocities of a nonlinear polarization and an exciting laser pulse are almost equal. Under SF, nonlinear optical processes including stimulated Raman scattering (SRS), stimulated Brillouin–Mandelstam scattering, generation of optical harmonics, *etc.*, occur under conditions, where the speed of the nonlinear polarization amplitude envelope is close to  $v_{\text{fp}}$  and does not depend on the group velocities of exciting and generated components. The speed  $v_{\text{fp}}$  of a self-focusing focal point is variable and could be controlled due to its dependence on the envelope shape and the exciting pulse amplitude. When there is no SF, the efficiency of nonlinear optical processes reaches its maximum at the equality of all phase and, consequently, group velocities of interacting and generated waves. But this condition is not always achieved. Due to new technology prospects, the efficiency of nonlinear optical processes under SF could be controlled even in a disperse medium and can be optimized by choosing  $v_{\text{fp}}$ .

However, the efficiency of nonlinear optical processes under SF is significantly affected by the self-modulation of the phase (SMP) of laser radiation, which alters the instantaneous frequency and the phase matching of interacting waves.

## 1. Introduction

Self-focusing (SF) of laser pulses in the nanosecond duration interval in various media, which are characterized by the essential Kerr effect, leads to the movement of a focal spot due to the instantaneous power change. The focal spot speed  $v_{\text{fp}}$  is defined by laser pulse envelope. The faster the change of the instantaneous power of a pulse, the greater is the speed  $v_{\text{fp}}$ . At the front and the back of a pulse, the speed  $v_{\text{fp}}$  takes both positive and negative values and is not limited by the speed of light in vacuum.

It was stated in [1] that the motion of a focal spot with a superluminal speed does not contradict the special theory of relativity, because the focal spot is created at different moments of time by SF of different time fragments of the input pulse. Therefore, the motion of a focal spot is not associated with the energy transfer. However, there is a strong polarization of the medium induced at the moving focus, which may have superluminal speed.

This paper analyzes the influence of a moving SF focal area on parametric anti-Stokes SRS with regard for SMP of laser radiation and anti-Stokes component (ASC) radiation, which is generated near the focal point [2] and propagates up to the medium boundary (to the observer) under a refractive index variable in space and time.

It was shown previously [3] that the frequency of ASC in an SRS-active medium depends on the focal point speed even in the approximation of "ideal thin lens", which implies that the instantaneous change of the laser pulse power leads only to a change of the focal length of the induced lens, while the SMP effect is considered insignificant. This situation can be rather easily realized, by varying the curvature radii of the additional lens, when there is no SF. However, the actual induced lens in an SF-medium varies its "thickness", which leads to a significant SMP of laser and ASC radiation.

The spectrum of self-modulated nanosecond laser pulses was theoretically and experimentally researched in [4]. When the focal point crosses the output boundary of the SF-medium at the front of a laser pulse, the spectral broadening of laser radiation exceeds  $100 \text{ cm}^{-1}$  to the side of lower frequencies. This is explained by the transient effect on the SF-medium boundary, which is somewhat similar to the physical mechanism of generation of a transient radiation [5]. When the Kerr medium boundary is crossed by the focal area, where the refractive index is increased and varies in time, the phases of electromagnetic fields change. The transient effect under SF can be used to adjust the frequency and to compress laser pulses [6].

The spectral broadening of laser radiation due to SMP in an SRS-active self-focusing medium leads to a spectral broadening of SRS, which occurs in focal areas of SF [2], i.e. near the focal point.

It was experimentally established [7] that the frequency ( $\omega$ ) – angular ( $\theta$ ) bands  $\omega(\theta)$  of various spectral broadenings are observed in the frequency-angular spectra of SRS ASC conical radiation. The dependence of the scattered radiation frequency  $\omega$  on the angle  $\theta$  is typically observed as parabolic frequency-angular bands of ASC  $\omega(\theta) - \omega_a \approx (\omega(\theta = 0) - \omega_a) (1 - \theta^2/\theta^2(\omega_a))$ , where  $\omega_a$  is the Raman anti-Stokes frequency, and  $\theta$  is the angle between the laser pulse propagation axis and a scattering direction of the conical radiation ( $\theta = 0$  corresponds to the axial scattering).

The Stokes shift in the mentioned bands is described by the relation similar to that for Cherenkov radiation [7]:  $\cos \theta(\omega) = v_{\text{ph}}(\omega)/v_{\text{ap0}}(\omega_a)$ , where  $v_{\text{ph}}(\omega)$  is the phase velocity of the ASC radiation with frequency  $\omega$ , which is scattered at an angle  $\theta$ ,  $v_{\text{ap0}}(\omega_a)$  is the phase

velocity of a nonlinear medium polarization wave at the frequency  $\omega_a$  with no SF. In case of normal dispersion, the speed  $v_{\text{ap0}}(\omega_a)$  becomes superluminal. When the frequencies are  $\omega = \omega_a$ , we obtain  $\cos \theta = k_{\text{ap0}}(\omega_a)/k(\omega_a)$ , where  $k_{\text{ap0}}$  and  $k$  are the lengths of the polarization and scattering wave vectors in the medium. This Cherenkov-type dependence at the anti-Stokes Raman frequency  $\omega_a$  has been noted earlier [8]. A similar dependence is also observed under the excitation by femtosecond laser pulses, in particular, focused using an axicon [9].

What's been left unexplained is the physical mechanism of generation of Cherenkov-type conical ASC radiation at non-Raman frequencies and its relation to the focal point speed and SMP of laser radiation. Work [7] shows only formally that the frequency-angular spectrum of experimentally observed broadband cone ASC radiation can be analytically described with satisfactory accuracy by the Cherenkov radiation condition  $\cos \theta(\omega) = v_{\text{ph}}(\omega)/v_{\text{ap0}}(\omega_a)$ , where the speed of a charged particle is replaced with the phase velocity  $v_{\text{ap0}}(\omega_a)$  of nonlinear polarization waves, which propagate in a medium at the frequency  $\omega_a$  in the absence of SF and SMP. This paper describes the physical mechanism that causes the generation of broadband (and angle-dependent) ASC radiation of Cherenkov-type in the SRS-active SF-medium.

The actuality of this work is determined by opportunities, which are almost not considered and are realizable due to a combination of SRS as an effective method of laser radiation frequency adjustment and SF, which gives an ability to perform the spatial scanning by electromagnetic field packages with unlimited and controllable speed. The SF focal point speed  $v_{\text{fp}}$  does not directly depend on the group velocity of an exciting pulse and the speed of light in vacuum [1]. This gives prospects to create new coherent radiation sources with frequency adjustment ability and with new frequency-angular properties. At the same time, the possibility to sweep laser radiation on a shifted frequency appears.

## 2. Analytical Consideration

The source of SRS ASC radiation is a wave of medium's nonlinear polarization  $P^{\text{NL}}(t, r)$ . The intensity of ASC depends both on the spatial-temporal distribution of the amplitude and on the phase of this wave, as it is necessary to achieve the phase matching with the anti-Stokes radiation field. At the same polarization of all waves in the electric dipole approximation in the case of a homogeneous non-magnetic and non-conducting medium, without regard for the reflection on the medium bound-

aries, the far-field frequency-angular energy density  $W_{\omega\theta}$  of ASC at small scattering angles  $\theta$  (within a few degrees) is defined by the formula [3]

$W_{\omega\theta} =$

$$= \frac{\omega^4 n_\omega}{8\pi^2 c^3} \left| \int_V dV \int_{-\infty}^{\infty} P^{\text{NL}}(t, \mathbf{r}) \exp[i(\omega t - \mathbf{k}\mathbf{r})] dt \right|^2, \quad (1)$$

where  $\mathbf{k}$  is a scattered radiation wave vector with a length of  $k = n\omega/c$  at the frequency  $\omega$ ,  $n = n(\omega)$  is the refraction index,  $c$  is the speed of light in vacuum,  $t$  is the time, and  $\mathbf{r}$  is a radius vector that connects the origin of the coordinate system and an arbitrary point of the volume  $V$ , where medium's nonlinear polarization exists. The physical meaning of formula (1) is based on the decomposition of a nonlinear polarization at every point of the volume in a set, which is continuous in frequency, of monochromatic radiation sources, followed by the spatial summation of the field emitted by these point sources. It also takes into consideration the phase of these sources and the phase of the emitted field, which arrives at the observation point.

To perform calculations of the frequency-angular energy density using formula (1), it is firstly necessary to determine only the spatial-temporal dependence of the amplitude and the phase of a polarization  $P^{\text{NL}}(t, \mathbf{r})$ . However, under SF and SMP, it is a very difficult task.

To simplify calculations, we will use the approximation of a given polarization. Let us assume that, when SF and SMP are neglected, the linearly polarized exciting laser radiation with wave vector  $\mathbf{k}_L$  (in the medium) and frequency  $\omega_L$  propagates along the axis  $\mathbf{z}$  and has phase  $\phi_L = \omega_L t - k_L z$ . The Stokes Raman component of SRS, which is excited by laser radiation, propagates in the same direction and has the wave vector  $\mathbf{k}_s$  and the frequency  $\omega_s$ . These two waves create the cubic polarization of a medium at the anti-Stokes Raman frequency  $\omega_a = 2\omega_L - \omega_s$  with a wave vector of  $\mathbf{k}_{\text{ap}0} = 2\mathbf{k}_L - \mathbf{k}_s$ . As  $\mathbf{k}_L$  and  $\mathbf{k}_s$  are oriented in the same direction, the vector  $\mathbf{k}_{\text{ap}0}$  is oriented along the axis  $z$  as well, and its length is  $k_{\text{ap}0} = 2k_L - k_s$ .

An increase of the refraction index  $\Delta n$  under SF causes the length  $k_L$  to increase up to  $\Delta k_L = k_L \Delta n/n$ , by creating, thus, a phase delay  $\delta\varphi_L(t, z)$  of laser radiation. Therefore, we obtain  $\varphi_L = \omega_L t - k_L z - \delta\varphi_L(t, z)$ . This delay depends on the instantaneous intensity of exciting radiation pulses, the distance, and, hence, on the

time  $t$  and the coordinate  $z$ , and is defined by expression:

$$\delta\varphi_L(t, z) = \int_{Z_{\text{in}}}^z \Delta k_L(t, \zeta) d\zeta. \quad (2)$$

Expression (2) assumes that the SRS-active self-focusing medium is located within  $z = Z_{\text{in}} \div L/2$  (henceforth, the coordinate  $z_f$  of the created focal point is considered in the range of  $z_f = -L/2 \div L/2$ , and  $Z_{\text{in}} \ll -L/2$ ),  $\zeta$  is a current integration coordinate on the path between the input boundary of the medium and a point  $z$ , where the phase is considered. The delay  $\delta\varphi_L$  can be calculated rather accurately, and it has been done in [4]. Here, to calculate the increase  $\Delta k_L(t, \zeta)$  of the laser radiation wave vector length, which is caused by an increase of the refraction index at every intermediate point  $\zeta$  of the path  $Z_{\text{in}} \div z$ , the following approximation is used:

$$\Delta k_L(t, \zeta) = \Gamma_f \exp \left[ - \left( \zeta - v_{\text{fp}} \left( t - \frac{z - \zeta}{v_g} \right) \right)^2 / b^2 \right]. \quad (3)$$

Here,  $\Gamma_f$  is the maximum increase of  $\Delta k_L$  at the center of the focal area (i.e. at the focal point),  $v_{\text{fp}}$  is the speed of the focal point, and its coordinate is  $z_f = v_{\text{fp}} t$  (we assume that the speed is constant and  $z_f(t=0) = 0$ ),  $v_g$  is the group velocity of light at a laser radiation frequency,  $b$  is the effective length of the focal area. Expression (3) indicates the situation, in which some time fragment of the laser pulse, located at  $z$  at  $t$ , was located at  $\zeta$  at  $t' = t - (z - \zeta)/v_g$ . The focal point coordinate at this moment of time was  $z'_f = v_{\text{fp}} t' = v_{\text{fp}} (t - (z - \zeta)/v_g)$ . Accordingly, the distance between the fragment and the focal point was  $\zeta - z'_f = \zeta - v_{\text{fp}} (t - (z - \zeta)/v_g)$ . In the case of the Gaussian distribution of the value of refractive index in the focal area, which is proportional to  $\exp \left[ - ((z - z_f)/b)^2 \right]$ , we obtain the required expression (3) for  $\Delta k_L(t, \zeta)$ .

The focal area is created near the output boundary of a medium. When  $L/2 \gg |Z_{\text{in}}|, b$ , we get  $\Delta k_L(t, \zeta) \approx 0$  at the input boundary. Therefore, the lower integration limit in (2) can be replaced by  $-\infty$ .

SRS mainly occurs at the center of an SF focal area. So, the behavior of the exciting laser radiation phase is especially important at the focal point. The substitution of  $z = v_{\text{fp}} t$  or  $t = z/v_{\text{fp}}$  into (2) and (3) gives

$$\delta\varphi_L(t, z = v_{\text{fp}} t) = \frac{\sqrt{\pi}}{2} b \Gamma_f \left| \frac{1}{1 - v_{\text{fp}}/v_g} \right|, \quad (4)$$

$$\left. \frac{\partial \delta \varphi_L}{\partial t} \right|_{z=v_{fp}t} = -\Gamma_f \frac{v_{fp}}{1 - v_{fp}/v_g}, \quad (5)$$

$$\left. \frac{\partial \delta \varphi_L}{\partial z} \right|_{z=v_{fp}t} = \Gamma_f \frac{1}{1 - v_{fp}/v_g}. \quad (6)$$

So, considering SF and SMP at the focal point, the frequency  $\omega_{Lf}$  and the length  $k_{Lf}$  of the laser radiation wave vector change and become

$$\omega_{Lf} = \left. \frac{\partial (\varphi_L)}{\partial t} \right|_{z=v_{fp}t} = \omega_L + \Gamma_f \frac{v_{fp}}{1 - v_{fp}/v_g}, \quad (7)$$

$$k_{Lf} = - \left. \frac{\partial (\varphi_L)}{\partial z} \right|_{z=v_{fp}t} = k_L + \Gamma_f \frac{1}{1 - v_{fp}/v_g}. \quad (8)$$

Using the first derivatives and the linear approximation near the focal point, we obtain the phase delay:

$$\begin{aligned} \delta \varphi_L(t, z) &= \delta \varphi_L(t, z_f = v_{fp}t) + \\ &+ \left. \frac{\partial \delta \varphi_L}{\partial t} \right|_{z=v_{fp}t} (t - z_f/v_{fp}) + \left. \frac{\partial (\varphi_L)}{\partial z} \right|_{z=v_{fp}t} (z - z_f) = \\ &= \frac{\sqrt{\pi}}{2} b \Gamma_f \left| \frac{1}{1 - v_{fp}/v_g} \right| - \Gamma_f \frac{v_{fp}}{1 - v_{fp}/v_g} t + \Gamma_f \frac{1}{1 - v_{fp}/v_g} z. \end{aligned} \quad (9)$$

The self-modulation of the phase of laser radiation is transferred to the Stokes component phase  $\varphi_s$  [9]. Therefore, the phase  $\varphi_{ap}$  of the nonlinear polarization  $P^{NL} = P_0^{NL} \exp(-i\varphi_{ap})$  of a medium at the anti-Stokes frequency can be represented in the form

$$\begin{aligned} \varphi_{ap} &= 2\varphi_L - \varphi_s = 2(\omega_L t - k_L z - \delta \varphi_L) - \\ &- (\omega_s t - k_s z - \delta \varphi_L) = \omega_a t - k_{ap} z - \delta \varphi_L. \end{aligned} \quad (10)$$

However, it is necessary to consider that the refractive index is also modified between the focal point and medium's output boundary. The waves emitted by the polarization at the frequency  $\omega$  change their phase by some value  $\delta \varphi_\omega(t, z)$  that depends on the radiation source coordinate and the time. Similar to how we obtained  $\delta \varphi_L(t, z)$ , we can write down the following expression for  $\delta \varphi_\omega(t, z)$ , when  $\theta = 0$ :

$$\delta \varphi_\omega(t, z) = \int_z^{L/2} \Delta k_\omega(t, \zeta) d\zeta,$$

$$\Delta k_\omega = \Gamma_f \exp \left[ - \left( \zeta - v_{fp} \left( t - \frac{z - \zeta}{v_{ph}} \right) \right)^2 / b^2 \right]. \quad (11)$$

The difference consists in that, instead of the group velocity  $v_g$  of light at the laser radiation frequency (a laser pulse fragment is moving at this speed), the phase velocity  $v_{ph}(\omega)$  of waves emitted at the frequency  $\omega$  appears, and the limits of integration are changed. Expressions (11) take into consideration that the phase front, which originated at a point  $z$  and the time  $t$ , will get to the point  $\zeta$ , which is located on the path from  $z$  to medium's output boundary (with the coordinate  $L/2$ ), at  $t'' = t + (\zeta - z)/v_{ph}$ . The focal point coordinate at that time moment will be  $z''_f = v_{fp}t'' = v_{fp}(t + (\zeta - z)/v_{ph})$ . The distance between the given phase front and the focal point will be  $\zeta - z''_f = \zeta - v_{fp}(t + (\zeta - z)/v_{ph}) = \zeta - v_{fp}(t - (z - \zeta)/v_{ph})$ , and it determines the refractive index at the point  $\zeta$ .

For sources at the focal point, where the polarization amplitude reaches its maximum, the phase delay

$$\delta \varphi_\omega|_{t=\frac{z_f}{v_{fp}}} = \Gamma_f \int_{z_f}^{L/2} \exp \left[ - \frac{(\zeta - z_f)^2}{b^2} \left( 1 - \frac{v_{fp}}{v_{ph}} \right)^2 \right] d\zeta. \quad (12)$$

Expression (12) indicates that  $\delta \varphi_\omega$  unlike  $\delta \varphi_L$  depends on the focal point coordinate and has a certain peculiarity at speeds  $v_{fp} = v_{ph}$ . By analyzing the behavior of  $\delta \varphi_\omega$  in the region  $v_{fp} \approx v_{ph}$ , we can use the interpolation  $\exp[-x^2] \approx 1 - x^2$  and obtain an analytical expression for  $\delta \varphi_\omega$  at the focal point:

$$\begin{aligned} \delta \varphi_\omega \Big|_{\substack{t = z_f/v_{fp} \\ v_{fp} \approx v_{ph}}} &= \\ &= \Gamma_f \left[ \left( \frac{L}{2} - z_f \right) - \frac{\left( \frac{L}{2} - z_f \right)^3 \left( 1 - \frac{v_{fp}}{v_{ph}} \right)^2}{3b^2} \right]. \end{aligned} \quad (13)$$

Under similar assumptions for derivatives, we have

$$\left. \frac{\partial (\delta \varphi_\omega)}{\partial t} \right|_{\substack{t = z_f/v_{fp} \\ v_{fp} \approx v_{ph}}} = \frac{\Gamma_f v_{fp}}{b^2} \left( \frac{L}{2} - z_f \right)^2 \left( 1 - \frac{v_{fp}}{v_{ph}} \right), \quad (14)$$

$$\left. \frac{\partial (\delta \varphi_\omega)}{\partial z} \right|_{\substack{t = z_f/v_{fp} \\ v_{fp} \approx v_{ph}}} =$$

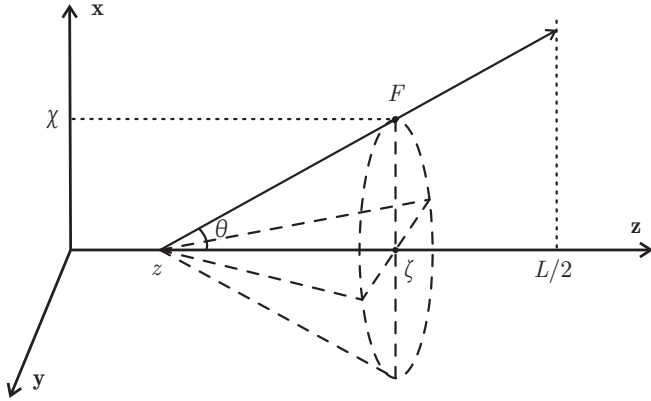


Fig. 1. Propagation of scattered radiation from a point  $z$  to the medium boundary

$$= -\Gamma_f \left[ 1 + \frac{v_{fp}}{v_{ph} b^2} \left( \frac{L}{2} - z_f \right)^2 \left( 1 - \frac{v_{fp}}{v_{ph}} \right) \right]. \quad (15)$$

Using the first derivatives and the linear approximation and by neglecting the terms proportional to  $(1 - v_{fp}/v_{ph})^2$ , we can represent the phase delay  $\delta\varphi_\omega$  near the focal point ( $z \approx z_f$ ) as

$$\delta\varphi_\omega = \Gamma_f \left[ L/2 + \left( v_{fp}(L/2 - z)^2 (1 - v_{fp}/v_{ph}) / b^2 \right) t - \left( 1 + \frac{v_{fp}}{v_{ph}} (L/2 - z)^2 (1 - v_{fp}/v_{ph}) / b^2 \right) z \right]. \quad (16)$$

To within permanent terms, the nonlinear polarization phase  $\varphi_{ap}$  with regard for both phase delays  $\delta\varphi_L$  and  $\delta\varphi_\omega$  and the correction  $k_{ap0} \rightarrow k_{ap0} + \Gamma_f$  (increase of the lengths of the wave vectors  $k_L$  and  $k_s$  at the focal point due to SF, but without SMP) takes form

$$\begin{aligned} \varphi_{ap} &= \omega_a t - k_{ap0} z - \delta\varphi_L - \delta\varphi_\omega = \\ &= \left( \omega_a + \frac{\Gamma_f v_{fp}}{1 - v_{fp}/v_g} - \Gamma_f v_{fp} \frac{(L/2 - z)^2 (1 - v_{fp}/v_{ph})}{b^2} \right) t - \\ &- \left( k_{ap0} + \frac{\Gamma_f}{1 - v_{fp}/v_g} - \Gamma_f \frac{v_{fp}}{v_{ph}} \frac{(L/2 - z)^2 (1 - v_{fp}/v_{ph})}{b^2} \right) z. \end{aligned} \quad (17)$$

We assume that the polarization amplitude  $P_0^{NL}$  reaches its maximum value at the focal point, while the amplitude distribution is Gaussian with the half-width  $b$  at the  $e^{-1}$  level along the  $z$  axis, and the half-width

$a_f$  along  $x$  and  $y$ . In this case, we obtain the following formula for the polarization amplitude:

$$P_0^{NL} = P_{0,\max}^{NL} \exp \left[ -\frac{x^2 + y^2}{a_f^2} - \frac{(z - v_{fp}t)^2}{b^2} \right]. \quad (18)$$

The polarization amplitude decline on the  $z$  axis at some distance from the point  $z_f$  allows us to use the linear approximation (17) for the phase delay, since the error in determining the polarization phase does not affect the obtained result due to a low polarization amplitude.

Substituting  $P^{NL} = P_0^{NL} \exp(-i\varphi_{ap})$  into (1) and performing the analytical integration with respect to  $t$ ,  $x$ , and  $y$  at the angle  $\theta = 0$ , we obtain the expression, which requires one to carry out the integration with respect to  $z$ :

$$\begin{aligned} W_{\omega\theta}(\theta=0) &= \frac{\pi n \omega^4 a_f^4 b^2}{4 v_{fp}^2 c^3} P_{0,\max}^{NL} \int_{-L/2}^{L/2} dz \exp \left[ \frac{b^2}{4 v_{fp}^2} \times \right. \\ &\times \left( \omega - \omega_a - \frac{\Gamma_f v_{fp}}{1 - v_{fp}/v_g} + \frac{\Gamma_f v_{fp}}{b^2} \left( \frac{L}{2} - z \right)^2 \left( 1 - \frac{v_{fp}}{v_{ph}} \right) \right)^2 - \\ &\left. - i \left( k - k_{ap0} - \frac{\omega - \omega_a}{v_{fp}} - \frac{\Gamma_f}{b^2} \left( \frac{L}{2} - z \right)^2 \left( 1 - \frac{v_{fp}}{v_{ph}} \right) \right) z \right]^2 \end{aligned} \quad (19)$$

The further calculations of the frequency-angular energy density can be performed only numerically.

The description of the ASC scattering at angles  $\theta \neq 0$  requires an additional refinement. To do this, we need to review expressions (11) once more. Let the scattered conical radiation propagate from a point  $z$  at the angle  $\theta$  (Fig. 1) in the plane  $\{x, z, y = 0\}$ , where the input slit of a registering spectrograph is located.

We assume that some phase front of the wave came out of a point  $z$  at the time moment  $t$ . The phase front at the point  $F$  (Fig. 1) takes the longitudinal coordinate  $\zeta$ , and its distances from the axis  $\mathbf{z}$  and the point  $z$  are, respectively,  $\chi = (\zeta - z) \operatorname{tg} \theta$  and  $\sqrt{(\zeta - z)^2 + \chi^2}$ . Thus, the front arrives at  $\zeta$  at  $t + \sqrt{(\zeta - z)^2 + \chi^2} / v_{ph} = t + (\zeta - z) / (v_{ph} \cos \theta)$ . At this moment, the focal point will take the coordinate  $v_{fp} (t + (\zeta - z) / (v_{ph} \cos \theta))$ . The distance between the front and the focal point will be  $\zeta - v_{fp} (t + (\zeta - z) / (v_{ph} \cos \theta))$  along the axis  $\mathbf{z}$  and  $(\zeta - z) \operatorname{tg} \theta$  along the axis  $\mathbf{x}$ . Thus, the increase of the

wave vector length at the point  $F$  (Fig. 1) takes the value

$$\Delta k_\omega = \Gamma_f \exp \left[ - \left( \frac{(\zeta - z) \operatorname{tg} \theta}{a_f} \right)^2 - \left( \frac{\zeta - v_{\text{fp}} \left( t + \frac{\zeta - z}{v_{\text{ph}} \cos \theta} \right)}{b} \right)^2 \right], \quad (20)$$

where  $a_f$  is the focal area radius at the  $e^{-1}$  level of changes in  $\Delta n$  and  $\Delta k_\omega$ .

In order to calculate the phase delay  $\delta\varphi_\omega$ , we integrate  $\Delta k_\omega$  with respect to  $\zeta$  within  $\{z \div L/2\}$ . The usage of expression (20) without additional approximations significantly complicates the procedure of obtaining an analytical expression for  $\delta\varphi_\omega$  at  $\theta \neq 0$ , which would be similar to (16).

An acceptable simplification would be the following representation of  $\delta\varphi_\omega$  for sources with maximum oscillation amplitude at the focal point:

$$\delta\varphi_\omega|_{t=\frac{z_f}{v_{\text{fp}}}} = \Gamma_f \int_{z_f}^{L_{z\theta}} \exp \left[ - \frac{(\zeta - z_f)^2}{b^2} \left( 1 - \frac{v_{\text{fp}}}{v_{\text{ph}} \cos \theta} \right)^2 \right] d\zeta. \quad (21)$$

Here, in comparison with (12), the speed  $v_{\text{ph}}$  is replaced by  $v_{\text{ph}} \cos \theta$ , and the upper integration limit  $L/2$  is replaced by the minimum value  $L_{z\theta} = \text{Min}[L/2; z + a_f \sqrt{\pi}/(2 \sin \theta)]$  of both specified values.

The possibility to use (21) has been tested by numerical calculations. From the physical point of view, expression (21) is a result of replacing the Gaussian distribution  $\Delta k_\omega$  along the axis  $x$  by a stepped distribution in the focal plane  $z = z_f$

$$\Delta k_\omega(x, y = 0 \div a_f) = \Gamma_f, \quad \Delta k_\omega(x, y > a_f) = 0$$

maintaining the resulting value  $\delta\varphi_\omega|_{t=z_f/v_{\text{fp}}}$  for the waves propagating from the focal point at the ratio of speeds  $v_{\text{fp}}/v_{\text{ph}}$  nearly equal to  $v_{\text{fp}}/v_{\text{ph}} \approx 1$ .

Expression (21) is identical to the previously obtained expression (12) after replacing  $L/2 \rightarrow L_{z\theta}$  and  $v_{\text{ph}} \rightarrow v_{\text{ph}} \cos \theta$ . Such substitutions allow the further use of results (16) and (17) in the case where  $\theta \neq 0$  and  $v_{\text{ph}} \approx v_{\text{ph}}$ .

In order to describe the frequency-angular structure of ASC scattering, it is important to consider the phase of waves generated within the entire focal area. We confine ourselves by the consideration of variations of  $\Delta n$  in the

focal plane, where the nonlinear polarization amplitude reaches its maximum. To use this approach, we need to perform the following replacement:

$$\Gamma_f \rightarrow \Gamma_f \exp \left( - \frac{x^2 + y^2}{a_f^2} \right).$$

Moreover, for angles  $\theta \neq 0$  in (1), we need to consider that  $\mathbf{k}\mathbf{r} = \Delta k_\perp x + \Delta k_\parallel z$ , where  $\Delta k_\perp = k \sin \theta$  and  $\Delta k_\parallel = k \cos \theta - k_{\text{ap}0}$ . After all corrections, which require the further numerical integration with respect to  $x$  and  $y$ , the frequency-angular energy density

$$W_{\omega\theta} = \frac{n\omega^4 b^2 P_{0,\text{max}}^{\text{NL}}}{8\pi v_{\text{fp}}^2 c^3} \left| \int_0^\infty dx \int_0^\infty dy \int_{-L/2}^{L/2} \exp \left[ - \frac{x^2 + y^2}{a_f^2} - ik_\perp x - \frac{b^2}{4v_{\text{fp}}^2} \left( \omega - \omega_a - \frac{\Gamma_f v_{\text{fp}}}{1 - v_{\text{fp}}/v_g} + \frac{\Gamma_f v_{\text{fp}}}{b^2} (L_{z\theta} - z)^2 \right) \times \left( 1 - \frac{v_{\text{fp}}}{v_{\text{ph}} \cos \theta} \right)^2 - i \left( \Delta k_\parallel - \frac{\omega - \omega_a}{v_{\text{fp}}} - \frac{\Gamma_f}{b^2} (L_{z\theta} - z)^2 \right) \times \left( 1 - \frac{v_{\text{fp}}}{v_{\text{ph}} \cos \theta} \right)^2 \right] dz \right|^2. \quad (22)$$

### 3. Calculation Results

Calculations have been performed for SRS in toluene, where the ASC Raman shift is  $(\omega_a - \omega_L)/2\pi c = 1004 \text{ cm}^{-1}$ . Data on the dependence  $n(\omega)$  have been taken from [11]. It was considered that  $a_f = 5 \mu\text{m}$  [1]. The optimal value of  $\Gamma_f$ , which depends on  $v_{\text{fp}}$  [12], was chosen as

$$\Gamma_{f,\text{opt}} \approx \frac{\Delta k_{\text{ap}0}}{1 - (1 - v_g/v_{\text{ga}})/(1 - v_g/v_{\text{ga}})},$$

where  $v_{\text{ga}}$  is the group velocity of light at the frequency  $\omega_a$ . The condition  $\Gamma_f = \Gamma_{f,\text{opt}}$  ensures the maximum generation efficiency of the anti-Stokes component. The typical value in toluene is  $\Gamma_{f,\text{opt}} \sim \Delta k_{\text{ap}0} = 46 \text{ cm}^{-1}$ .

Figure 2 presents dependence (19) of the peak energy density of axial anti-Stokes radiation  $W_{\omega\theta}^{(\text{max})}$  on the focal area speed at  $b = 0.1 \text{ cm}$  and various values of  $L$ : a)  $L = 1 \text{ cm}$ , b)  $L = 2 \text{ cm}$ , c)  $L = 3 \text{ cm}$ .

The energy density is given in relative units. The maximum  $W_{\omega\theta}^{(\text{max})}$  is at the focal area speed  $v_{\text{fp}} = 0.67c$ .

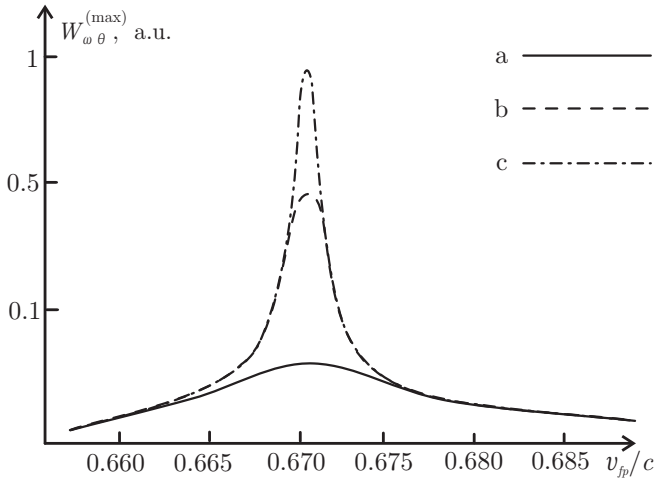


Fig. 2. Dependence of the peak energy density of axial anti-Stokes radiation component on the focal area speed  $v_{fp}$  at  $b = 0.1$  cm and various values of  $L$ : a)  $L = 1$  cm, b)  $L = 2$  cm, c)  $L = 3$  cm

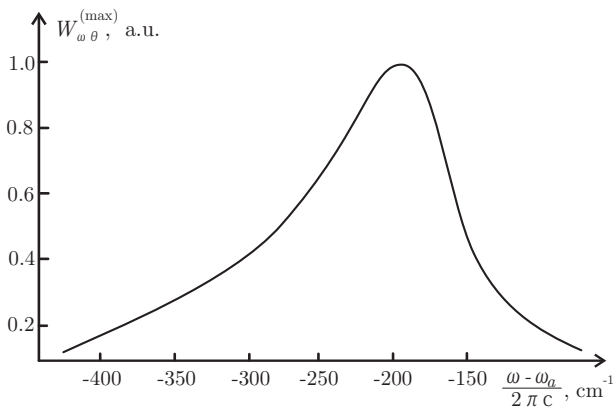


Fig. 3. Dependence of the axial anti-Stokes component peak energy density on the frequency shift at  $b = 0.1$  cm and  $L = 1$  cm

Even small deviations from this speed lead to a significant reduction in the energy density. As the length  $L$  of a self-focusing region, where the focal area propagates, of the medium increases, the narrowing of the allowable range of speeds is observed.

The speed of the focal area determines the location of the anti-Stokes radiation peak energy in the frequency spectrum. Figure 3 presents the dependence of the peak energy density (in dimensionless units) on the frequency shift  $(\omega - \omega_a)/2\pi c$  relative to the anti-Stokes Raman frequency.

The maximum value of peak energy density is observed at the radiation frequency, whose phase velocity matches the focal area speed:  $v_{ph} = v_{fp} = 0.67c$ ,  $(\omega - \omega_a)/2\pi c = -197 \text{ cm}^{-1}$ .

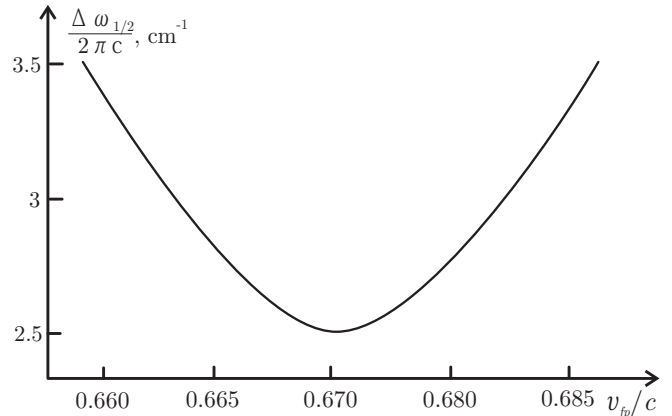


Fig. 4. Dependence of the radiation spectrum width on the focal area speed ( $b = 0.1$  cm and  $L = 1$  cm)

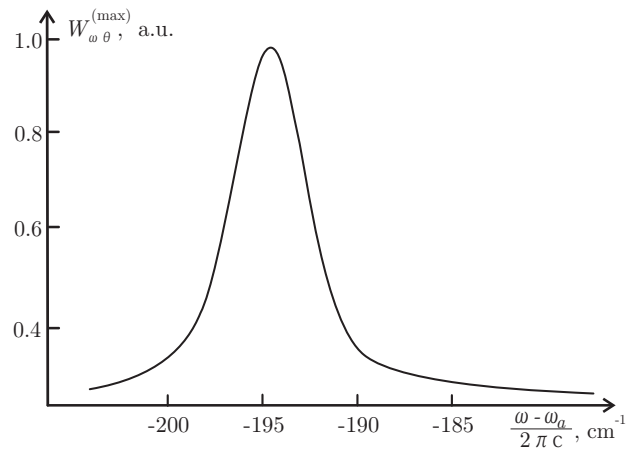


Fig. 5. Axial anti-Stokes component radiation spectrum at  $v_{fp} = 0.67c$

Figure 4 shows the dependence of the ASC spectrum width on the focal area speed. The minimum spectrum width is obtained, when  $v_{fp} = 0.67c$ , and is about  $2.5 \text{ cm}^{-1}$  at  $L = 1$  cm and  $b = 0.1$  cm.

The axial ASC spectrum at the speed  $v_{fp} = 0.67c$  is shown in Fig. 5. The maximum energy is observed at the frequency  $(\omega - \omega_a)/2\pi c = -197 \text{ cm}^{-1}$ .

These dependences are obtained using expression (19) for axial radiation. The full frequency-angular distribution  $W_{\omega\theta}$  of the ASC radiation energy is described by expression (22). The calculated frequency-angular band location at  $v_{fp} = 0.67c$ ,  $L = 1$  cm, and  $b = 0.1$  cm is shown in Fig. 6 as a solid line. The dashed line is provided as a comparison to the experimental dependence taken from [7]. The theoretical curve reaches  $-197 \text{ cm}^{-1}$  to the Stokes side, while the experimental one extends

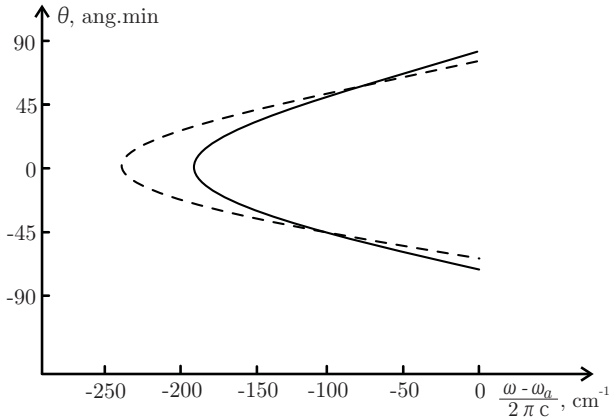


Fig. 6. Frequency-angular bands of the anti-Stokes radiation component: solid line for the theoretical result ( $v_{fp} = 0.67c$ ,  $L = 1$  cm,  $b = 0.1$  cm); dashed line for the experimental band

down to  $-235 \text{ cm}^{-1}$ . For angles, we have  $\pm 86'$  and  $\pm 71'$ , respectively.

The angular cross-sections of the theoretical distribution  $W_{\omega\theta}$  at several frequency shifts are shown on Fig. 7.

#### 4. Analysis of Results and Conclusions

The study shows that frequency-angular energy density of ASC, whose photon energy exceeds the energy of exciting photons, greatly depends on the SF focal point speed in SRS-active Kerr liquids. Under certain conditions, the frequency-angular indicatrix of the Cherenkov-type radiation is created with high efficiency:  $\cos\theta(\omega) \approx v_{ph}(\omega)/v_{ap0}(\omega_a)$ . We note that the indicatrix and the energy of actual Cherenkov radiation is completely described with the use of (1). The detailed description can be found in [13].

Two facts are important in the formation of the frequency-angular indicatrix of ASC. First of all, SMP of exciting laser radiation leads to the creation of anti-Stokes nonlinear polarization in a medium at the frequency and the phase velocity, which are shifted relative to Raman values with no SF. Considering this fact, the spectrum of ASC is described in [14]. At certain values of focal point speed, the equally significant role is played by SMP of ASC itself on the path from the focal area to the medium boundary. The optical length of this path depends on the ASC phase velocity and the focal point speed. Any change of the optical path in time causes the Doppler effect. An alternative and more appropriate way is the consideration of the optical path change based on the SMP effect.

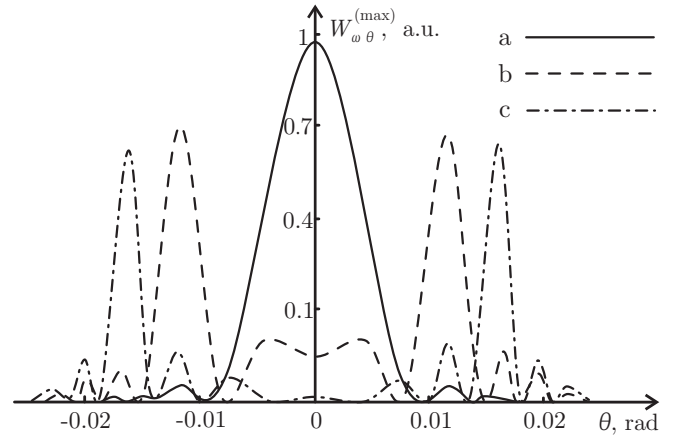


Fig. 7. Angular dependences of the anti-Stokes component energy density at  $v_{fp} = 0.67c$ ,  $L = 1$  cm,  $b = 0.1$  cm and frequency shifts: a)  $-197 \text{ cm}^{-1}$ , b)  $-150 \text{ cm}^{-1}$ , c)  $-110 \text{ cm}^{-1}$

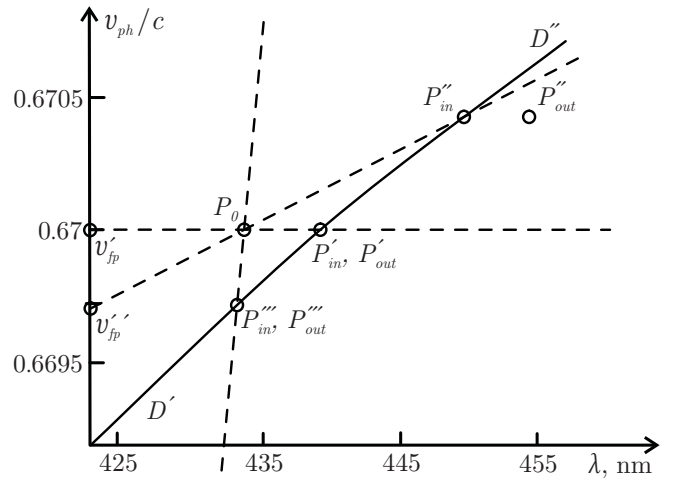


Fig. 8. Ehrenfest diagram for toluene ( $\theta = 0$ )

The explanation of the mutual influence of these factors is possible with the use of the Ehrenfest diagram [15], where the axes represent the wavelengths  $\lambda$  (in the medium) and the phase velocities  $v_{ph}(\lambda)$  of these waves. The analysis of the Ehrenfest diagram shows the basic regularities in the creation of broadband SRS ASC radiation in a SF-medium. The diagram for toluene, where  $\omega_a/2\pi c = 1004 \text{ cm}^{-1}$ , at the angle  $\theta = 0$  (axial scattering) is shown in Fig. 8.

Without regard for changes in the refractive index, the nonlinear ASC polarization takes coordinates  $P_0\{\lambda_{ap0}, v_{ap0}\}$  on the diagram, which are:  $\lambda_{ap0} = 2\pi/k_{ap0}$ ,  $v_{ap0} = \omega_a/k_{ap0}$ . Due to the dispersion of the refractive index, the coordinates  $P_0$  do not lie on the dispersion curve  $D'D''$  representing free electromagnetic

waves in a medium. The phase velocity  $v_{ap0}$  exceeds the speed of free electromagnetic waves of the same wavelength, and thus it becomes superluminal in the medium.

Temporal changes in the laser light optical path on the way to the SF focal point cause SMP and, therefore, change the frequency, wavelength, and phase velocity of the generated nonlinear polarization. In view of the SMP of laser radiation on the way to the focal point, the nonlinear ASC polarization takes new coordinates. At the speeds  $v'_{fp} = v_{ap0}$ ,  $v''_{fp} = 0.985v_{ap0}$ , and  $v'''_{fp} \rightarrow 0$ , which are chosen on the diagram, the coordinates of the polarization at the focal point center become  $P'_{in}$ ,  $P''_{in}$ ,  $P'''_{in}$ . These coordinates are determined by the focal point speed and the induced refractive index, which is related to  $\Gamma_f$ . For example, at  $P'_{in}\{\lambda, v_{ph}\}$  with regard for (9) and (10), we obtain

$$P'_{in} \left\{ \begin{array}{l} 2\pi / \left( k_{ap0} + \Gamma_f \frac{1}{1-v'_{fp}/v_g} \right), \\ \left( \omega_a + \Gamma_f \frac{v'_{fp}}{1-v'_{fp}/v_g} \right) / \left( k_{ap0} + \Gamma_f \frac{1}{1-v'_{fp}/v_g} \right) \end{array} \right\}.$$

The polarization coordinates  $P'_{in}$ ,  $P''_{in}$ , and  $P'''_{in}$  in the diagram lie on lines  $v'_{fp} \div P_0$ ,  $v''_{fp} \div P_0$ , and  $v'''_{fp} \div P_0$ , accordingly. This is caused by that the shifts  $\delta\omega_{in} = \omega_{Lf} - \omega_L = \Gamma_f v_{fp} / (1 - v_{fp}/v_g)$  of the anti-Stokes polarization frequency and  $\delta k_{in} = k_{Lf} - k_L = \Gamma_f / (1 - v_{fp}/v_g)$  of the wave vector length due to SMP on the way to the focal point are connected by the ratio  $\delta\omega_{in}/\delta k_{in} = v_{fp}$ . The change of  $\Gamma_f$  causes the polarization coordinates  $P'_{in}$ ,  $P''_{in}$ , and  $P'''_{in}$  to shift, but these coordinates are kept on the corresponding lines. The increase of  $\Gamma_f$  moves  $P'_{in}$ ,  $P''_{in}$ , and  $P'''_{in}$  away from  $P_0$ . At the zero value of  $\Gamma_f$ , we obtain  $P'_{in} = P''_{in} = P'''_{in} = P_0$ . When the optimum values of  $\Gamma_{f,opt}$  are achieved, the coordinates  $P'_{in}$ ,  $P''_{in}$ , and  $P'''_{in}$  lie on the dispersion curve  $D'D'$ , as shown in Fig. 8. In this case, the condition of amplitude-phase matching [3] (focal point speed, at which the polarization amplitude is maximal, matches the mutual group velocity of a polarization wave and a free electromagnetic wave) is satisfied, as well as the conditions of phase and group matching. If  $\Gamma_f(a_f, \dots) \neq \Gamma_{f,opt}$ , then only the amplitude-phase matching condition is satisfied. The peculiarities are observed only at the speed  $v'_{fp}$ . For this speed at arbitrary  $\Gamma_f$ , the amplitude-phase matching is obtained, and the phase velocity of polarization is equal to that of free electromagnetic waves.

The consideration of SMP at the focal area output changes the situation, but this depends on the speed  $v_{fp}$ . At speeds  $v'_{fp} = v_{ap0}$  and  $v'''_{fp} \rightarrow 0$ , the corresponding coordinates of the polarization  $P'_{out}$  and  $P'''_{out}$  in the

diagram remain unchanged. At other  $v_{fp}$ , for example  $v''_{fp} = 0.985v_{ap0}$  shown in Fig. 8, the coordinate of the polarization  $P''_{out}$  depends on  $(L/2 - z)$  i.e. on the location  $z = v''_{fp}t$  of the focal point and the boundary  $L/2$  of medium. The focal point movement leads to a shift  $P''_{out}$ , which is roughly parallel to the axis  $\lambda$ . This occurs because the frequency shift of the anti-Stokes polarization

$$\delta\omega_{out} = -\Gamma_f v''_{fp} (L/2 - z_f)^2 (1 - v''_{fp}/v_{ph}) / b^2$$

and the wave vector length

$$\delta k_{out} = -\Gamma_f v''_{fp} (L/2 - z_f)^2 (1 - v''_{fp}/v_{ph}) / (v_{ph} b^2)$$

are connected by the relation  $\delta\omega_{out}/\delta k_{out} = v_{ph}$  due to SMP on the way from the focal point to the medium boundary. The coordinate  $P''_{out}$  in Fig. 8 is drawn at  $L = 2.5$  cm,  $b = 0.25$  mm, and the optimum value  $\Gamma_f = 27.5$  cm<sup>-1</sup>.

It is worth noting that the frequency and the wave vector length of the nonlinear polarization at the focal point do not depend, in fact, on SMP of free electromagnetic waves on the way to the medium boundary. The given interpretation is based on the consideration of the observed polarization properties at the medium output. An alternative description considers the same changes of  $\delta\omega_{out}$ ,  $\delta k_{out}$  for free electromagnetic waves, but with opposite sign. In ant case, we obtain a shift in the diagram (Fig. 8) along the axis  $\lambda$  at  $P''_{out}$ .

The  $P''_{out}$  shift in the case where the focal point movement prevents the efficient up-conversion into ASC and the creation of pronounced peaks of the frequency-angular energy density  $W_{\omega\theta}$ . In this case, the phase matching of electromagnetic waves is not achieved in the plane, where the registration occurs, from different parts of the focal point path. Neither the amplitude-phase matching nor the phase and group ones are achieved for  $v''_{fp}$  along the whole path of the SF focal point.

In a range where  $v_{fp}$  is close to the phase velocity of light in a medium, there is a clear maximum, which is achieved at focal point speed  $v'_{fp} = v_{ap0}$ , which is equal to the phase velocity of light at the nonlinear polarization frequency at the focal point and the phase velocity of the polarization itself.

In this case, SMP of laser radiation, which enters the focal point, shifts the nonlinear polarization frequency, but does not affect its phase velocity; the phase velocity of polarization remains the same as in the absence of SF. On the other hand, SMP of ASC radiation at the focal area out has no effect on the frequency or the phase velocity of radiation.

The maximum energy density of axial ASC radiation is located at a frequency determined by conditions, which are similar to the conditions of Cherenkov radiation: the equality of the phase velocity of electromagnetic waves at the frequency  $\omega$  and the phase velocity of polarization at the anti-Stokes Raman frequency  $\omega_a$ . The frequency shift in toluene is  $(\omega(\theta=0) - \omega_a)/2\pi c = -197 \text{ cm}^{-1}$ .

At  $\theta \neq 0$  and  $v_{\text{fp}} = v_{\text{ap}0}$ , the frequency-angular bands are described by the relation

$$\cos \theta(\omega) \approx v_{\text{ph}}(\omega)/v_{\text{ap}0},$$

which gives parabola in the approximation  $\cos \theta \approx 1 - \theta^2/2$ :

$$\omega(\theta) - \omega_a \approx (\omega(\theta=0) - \omega_a) (1 - \theta^2/\theta^2(\omega_a)).$$

By this expression, the amplitude-phase matching is achieved for arbitrary changes of the refractive index at the focal area. At the optimum values  $\Gamma_{\text{f, opt}}(x, y, z)$  of  $\Delta k_{\text{L}}$ , the equality of longitudinal axis projections of the wave vectors of polarization and the ASC wave is ensured, which is important under conditions of significant lateral limitation of the area, where the nonlinear polarization exists under SF.

The theoretical results obtained are in agreement with experimental data. The presence of differences is discussed in [7].

Briefly summarizing, we determine the possible relation between the indicatrices of SRS ASC under SF and of Cherenkov radiation.

The frequency-angular energy density of both processes is described by (1), and they occur under a significant lateral limitation of the area, where the polarization exists.

The source of Vavilov–Cherenkov radiation is the polarization (volume density of dipole moment) created due to a change in the location of a free electron with charge  $q$  and speed  $v_q$ . The polarization of a medium is not taken into account, when describing the Vavilov–Cherenkov effect. Due to the motion of an electron, the spectral component of the polarization  $P_\omega = \int_{-\infty}^{\infty} P(t, \mathbf{r}) \exp[i(\omega t)] dt$  at the frequency  $\omega$  is characterized by the wave vector length  $\omega/v_q$  and phase velocity  $\omega/(\omega/v_q) = v_q$  on axis  $z$ , since [13]

$$P_\omega(x=0, y=0) = \frac{iq}{2\pi\omega} \exp\left(\frac{i\omega z}{v_q}\right).$$

The source of ASC radiation is a nonlinear medium polarization at the focal area. When  $v_{\text{fp}} = v_{\text{ap}0} = \omega_a/k_{\text{ap}0}$ ,

the spectral components of the observed ASC polarization at the frequency  $\omega$  in the focal area are described by the formula

$$P_\omega \sim \exp\left[-\frac{b^2}{4v_{\text{fp}}^2} \left(\omega - \omega_a - \frac{\Gamma_{\text{f}} v_{\text{fp}}}{1 - v_{\text{fp}}/v_g}\right)^2\right] \times \\ \times \exp[i((\omega - \omega_a)/v_{\text{fp}} + k_{\text{ap}0})z].$$

This expression shows that the wave vector length of spectral components of the polarization is equal to  $(\omega - \omega_a)/v_{\text{fp}} + k_{\text{ap}0} = \omega/v_{\text{ap}0}$ , and their phase velocities are  $v_{\text{ap}0}$ .

Therefore, under a significant lateral limitation of the area, where the nonlinear polarization exists, SRS ASC is described by the relation

$$\cos \theta(\omega) = v_{\text{ph}}(\omega)/v_{\text{ap}0},$$

which is similar to the Cherenkov radiation condition

$$\cos \theta(\omega) = v_{\text{ph}}(\omega)/v_q.$$

1. Y.R. Shen, *The Principles of Nonlinear Optics* (Wiley, New York, 2002).
2. A.I. Ivanisik, V.I. Maliy, and G.V. Ponezha, *Opt. and Spectrosc.* **80**, 212 (1996).
3. A.I. Ivanisik and G.V. Ponezha, *Opt. and Spectrosc.* **90**, 699 (2001).
4. S.O. Dudka, A.I. Ivanisik, A.V. Konopatskiy, and P.A. Korotkov, *Ukr. Phys. J.* **51**, 140 (2006).
5. V.L. Ginzburg, *Uspekhi Fiz. Nauk* **171**, 1097 (2001).
6. A.I. Ivanisik and A.V. Konopatskiy, *Visn. Kyiv. Univ. Ser. Fiz.-Mat. Nauki* **1**, 244 (2007).
7. A.I. Ivanisik, V.I. Maliy, and G.V. Ponezha, *Opt. and Spectrosc.* **82**, 447 (1997).
8. V.N. Lugovoy and A.M. Prokhorov, *JETP* **69**, 84 (1975).
9. I. Blonskyi, V. Kadan, I. Dmitruk, and P. Korenyuk, *Appl. Phys. B* **104**, 951 (2011).
10. A.P. Sukhorukov, *Nonlinear Wave Interactions in Optics and Radiophysics* (Nauka, Moscow, 1988) (in Russian).
11. A.I. Ivanisik, V.I. Maliy, and G.V. Ponezha, Available from UkrNIINTI **615-Uk85** (Kyiv, 1985).
12. A.I. Ivanisik and A.V. Konopatskiy, *Visn. Kyiv. Univ. Ser. Fiz.-Mat. Nauki* **3**, 331 (2006).
13. O.Iu. Isaienko and A.I. Ivanisik, in *Proc. of the XI-th International Young Scientists' Conference on Applied Physics* (T. Shevchenko Nat. Univ. of Kyiv, Kyiv, 2011), p. 19.
14. O.Iu. Isaenko and A.I. Ivanisik, *Visn. Kyiv. Univ. Ser. Fiz.-Mat. Nauki* **4**, 221 (2010).

15. D.V. Sivukhin, *Optics* (Nauka, Moscow, 1985) (in Russian).

Received 08.06.12

ФАЗОМОДУЛЬОВАНЕ ПАРАМЕТРИЧНЕ  
АНТИСТОКСОВЕ ВИМУШЕНЕ КОМБІНАЦІЙНЕ  
РОЗСІЯННЯ ЧЕРЕНКОВСЬКОГО ТИПУ  
В ОБЛАСТЯХ САМОФОКУСУВАННЯ  
ЗБУДЖУЮЧОГО ВИПРОМІНЮВАННЯ

*A.I. Іванісік, O.Ю. Ісаєнко, П.А. Коротков, Г.В. Понєжа*

Резюме

Розглянуто вплив швидкості руху фокальної точки самофокусування та фазової самомодуляції на частотно-кутові спе-

ктри випромінювання параметричної антистоксової компоненти вимушеного комбінаційного розсіяння. Враховано фазову самомодуляцію як збуджуючого, так і розсіяного антистоксового випромінювання. Пояснено утворення протяжних антистоксових частотно-кутових смуг. У випадку збігання швидкості фокальної точки самофокусування з фазовою швидкістю нелінійної поляризації на антистоксовій комбінаційній частоті та фазовою швидкістю розсіяного осевого випромінювання утворюються найінтенсивніші частотно-кутові смуги, які описуються співвідношеннями, характерними для черенковського випромінювання. Зокрема, за збудження наносекундними лазерними імпульсами в толуолі такі смуги сягають довжини  $\approx -200 \text{ см}^{-1}$  відносно комбінаційної антистоксової частоти.